Sensors and Actuators A 315 (2020) 112333

Contents lists available at ScienceDirect

Sensors and Actuators A: Physical

journal homepage: www.elsevier.com/locate/sna

Colossal photosensitive boost in Schottky diode behaviour with Ce-V_2O_5 interfaced layer of MIS structure

V. Balasubramani [a], J. Chandrasekaran [a,*], Tien Dai Nguyen [b,c], S. Maruthamuthu [d], R. Marnadu [a], P. Vivek [a], S. Sugarthi [e]

[a] Sri Ramakrishna Mission Vidyalaya College of Arts and Science, Coimbatore 641 020, Tamil Nadu, India
[b] Institute of Theoretical and Applied Research, Duy Tan University, Hanoi, 100000, Viet Nam
[c] Faculty of Natural Sciences, Duy Tan University, Da Nang, 550000, Viet Nam
[d] Department of Physics, PSG Institute of Technology and Applied Research, Coimbatore 641 062, Tamil Nadu, India
[e] SRM Institute of Science and Technology, Chennai 603 203, Tamil Nadu, India

ARTICLE INFO

Article history:
Received 15 June 2020
Received in revised form 12 August 2020
Accepted 6 September 2020
Available online 15 September 2020

Keywords:
Photo diode;photo detector
Thin films
MIS type Schottky barrier diodes
Spin coating

ABSTRACT

In the present work, we have fabricated a highly photo responsive Schottky barrier diode based on cerium infused vanadium pentoxide thin film (Ce-V_2O_5) as a interfacial layer. It was coated on a glass slide by low-cost sol-gel spin-coating technique and annealed at 500 °C. Structure, surface morphology, optical and electrical characteristic of Ce infused V_2O_5 films with different Ce concentrations *viz* 0, 2, 4 and 6 wt% were investigated. X-ray diffraction (XRD) pattern exposed that all coated films are tetragonal structure. And a peak shift was recorded after doping Ce ion into the V_2O_5 system. FE-SEM images showed a smooth nanorods and nanoplate-like structures in nano-scale region. Topology view by AFM showed a significant decrease in surface roughness of the film at different wt.% of Ce. The incorporation of Ce concentration based on the optical absorbance and band gap energy were studied, using UV–vis spectroscopy. Current-voltage (I–V), characteristics, photo-diode parameters of the Cu/Ce-V_2O_5/n-Si diodes were evaluated under dark and light exposed conditions. A maximum quantum efficiency of 25.54 % was achieved for the MIS diode fabricated with 6 % of Ce. The photosensitivity of the Cu/Ce-V_2O_5/n-Si diode 100 times higher than pure diode. Photodiode parameters and I–V analysis revealed that Ce with 6 wt.% is appropriate for the development of high quality photodiode and photo detector applications based to its electrical-performance.

1. Introduction

The Schottky barrier diode is an active electronic component that is widely used in modern optoelectronic application as light emitting diodes, laser diode, photo detectors, RF applications as a mixer or detector etc., It is used in power applications as a rectifier, because of it has low forward voltage drop and lesser power loss when compared to ordinary PN junction diodes.

Metal-insulator-semiconductor based Schottky devices have abundant importance due to their unique electrical, optical and structural properties. The interfacial layer between metal and semiconductor contact plays a dominant role in the device performance which provides, low forward voltage drops, stability and consistency. So far, different molybdenum trioxide (MoO_3), tungsten trioxide (WO_3) and vanadium pentoxide (V_2O_5), have been used as interfacial layer with exertion, to improve the schottky diode performance [1].

The V_2O_5 thin films play as a vital role in various electronic applications and has attracted more researchers over the past decades. They possess high work function, good transparency, wide optical band gap, different oxidation states V^{2+}, V^{3+}, V^{4+} and V^{5+}, layered structure, good chemical and thermal stability and excellent thermoelectric and electro chromic properties [2]. V_2O_5 is a prominent material for different device applications such as gas sensors, electronic devices, optical switching devices, organic field effect transistors, reversible cathode materials for Li batteries, Schottky diodes and particularly in photovoltaics [2]. The aim of the current work is to improve the photosensitivity of the MIS diode, so that it can be used as a interfacial layer for photo diode application.

Generally, rare earth metal ions effectively improve the electrical as well as optical properties. Rare earth elements like europium (Eu), gadolinium (Gd), yttrium (Y), neodymium (Nd), samarium

* Corresponding author.
E-mail address: jchandaravind@yahoo.com (J. Chandrasekaran).

https://doi.org/10.1016/j.sna.2020.112333
0924-4247/

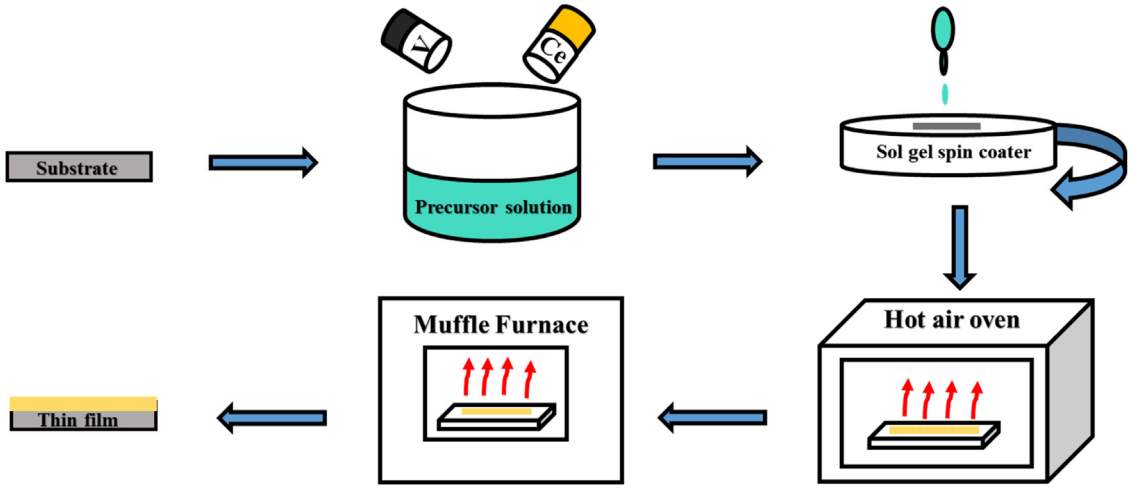

Fig. 1. Thin Film Deposition process.

(Sm), praseodymium (Pr) and cerium (Ce) increase the optoelectrical behaviours. In addition, rare-earth elements have much ability to absorb external light at shorter wavelength and emit at a longer wavelength, which increases the material trans-parency [3]. Among these, rare earth elements cerium oxide exists in both Ce^{3+} and Ce^{4+} oxidation state due to the sites occupied in matching host lattice. It is a potential candidate for photodiode applications owing to its high photo luminescent properties. Previously, phase transition and surface morphology effects on optical and electrical behaviour of nanostructed Ce doped V_2O_5 thin films have been investigated by B. Etemadi et al. [4]. Effect of Ce on Zno thin films and Schottky diode fabricated by a two-step chemical bath deposition exhibited adaptable proeperties which has been studied widely by M.A.M. Ahmeda et al. [5]. Besides, Marnadu et.al used Ce as a dopant material and they achieved a very high photosensitivity of 17,509.62 % [6]. To the best of our knowledge, there has been no work on the Ce doped vanadium thin films prepared by spin technique for MIS Schottky diode for photo detector applications.

The available thin film coating techniques are physical vapour deposition, electron beam evaporation, magnetron sputtering, pulsed laser deposition and some solution based techniques such as spray pyrolysis, spin coating and electro spinning technique. [2,7]. The sol-gel spin coating has been used in this work to deposit uniform thin films on flat substrate. It is a low temperature process and it gives a highly transparent coating which is also thermally stable. Furthermore, spin coated films have good electrochemical properties [7].

The objective of the present work is to prepare a high quality V_2O_5 thin films and incorporate Ce ions into the V_2O_5 matrix with various concentration viz 2, 4 and 6 wt%. Through sol-gel spin coating technique. The prepared films were used as interfacial layer in between metal and semiconductor interface to develop the MIS Schottky barrier diodes. Also, the I–V performance of the MIS diode were evaluated under dark and light conditions. Various photo-diode parameters were calculated and discussed in detailed.

2. Experimental details and characterization

All chemicals (vanadium chloride (VCl_3), cerium (iii) chloride ($CeCl_3$) and triton X-100) were purchased from sigma Aldrich. The precursor solution was prepared separately by dissolving vanadium chloride (0.2 M) in 5 mL of solvent (ethanol was used solvent) and stirred well. After 4 h, 2 mL of triton X-100 added individually in each solution and stirred well for 48 h continuously with the help of magnetic stirrer. The above trend was followed for the preparation of Ce doped V_2O_5 for various concentration 2, 4 and 6 wt%. The prepared solutions were meticulously coated on the well cleaned glass substrates at room temperature using programmable spin coater. The optimized 2500 rpm was fixed for all the films preparation. The coated films were dried at 100 °C for 15 min using a hot air oven. Finally, the prepared films were annealed at an optimized temperature of 500 °C for 1 h using high temp muffle furnace. This process was explained in Fig. 1.

Besides the MIS structured diodes was fabricated using single side polished n-Si (100) wafers of 1cm × 1cm in size with resistivity of 0–60 Ω-cm and 279 ± 25 μm thickness. The wafers were carefully cleaned to remove dust, grease and metallic impurities from the surface, which otherwise may lead to a lot of defects on the surface. The presence of defects and impurities can disturb the performance of MIS junction diode. The steps involved in cleaning are listed in the previous report [13]. Pure and Ce doped V_2O_5 solution was coated on Si substrate using the spin coating technique. The Schottky contact Cu was made on the Ce-V_2O_5/n-Si surface by DC sputtering technique through a shadow mask with high purity of copper target Cu, 99.99 % thickness of metal contact is 500 mm and diameter 4 mm. A non-rectifying junction called ohmic contact is made, by silver paste (Ag) on the rough side of the n-Si substrate and on the upper side of metal contact sides of the fabricated device and then it was to dry for 4 h at room temperature. Ag past, has a very good adhesive nature, high electrical conductivity with a sheet resistance with good solderability. A schematic illustration of the fabricated Cu/Ce-V_2O_5/n-Si device has been shown in Fig.12 (a).

First, the quality of the prepared pure V_2O_5 and Ce-V_2O_5 thin films were analysed by Rigaku Miniflex-II (CuK_α, λ = 1.5418 A) with the diffraction range of (10–80°). Stylus Profilometer detector (model: SJ-30) was used to measure the thickness of the film. Atomic force microscopy (model: 5100 Pico LE) and Field emission scanning electron microscope (Zeiss Sigma model: FEI quanta 250) was used to analyz the surface and morphological behaviour of Ce-V_2O_5 films. The existence of elements like V, O and Ce have been determined by energy dispersive X-ray analysis (EDX). The optical property was studied using UV–vis Spectrometer (JASCO, model: V-770PC). Finally, the electrical properties of the prepared thin films have been determined using two probe instruments at various temperature (30–150 °C). Keithley electro-meter (Model: 6517B) was used to study the current Vs voltage (I–V) characteristics of the fabricated Cu/Ce-V_2O_5/n-Si diode. The photo diode property of the diode was analysed by portable solar stimulator (PEC-L01) at 100 W/m^2 intensity.

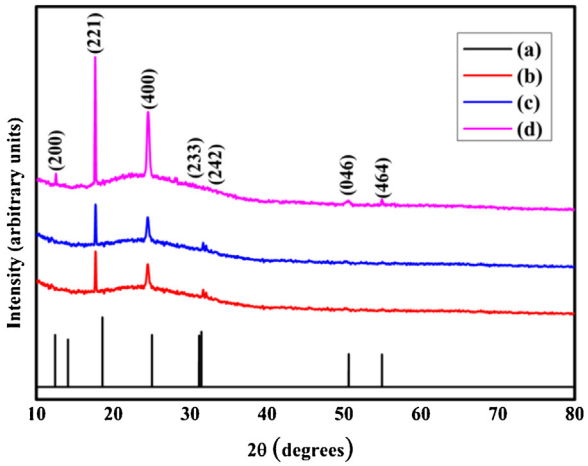

Fig. 2. XRD illustrate graph of (a) ICDD pattern (b-d) doped Ce-V_2O_5 (x) wt. %.

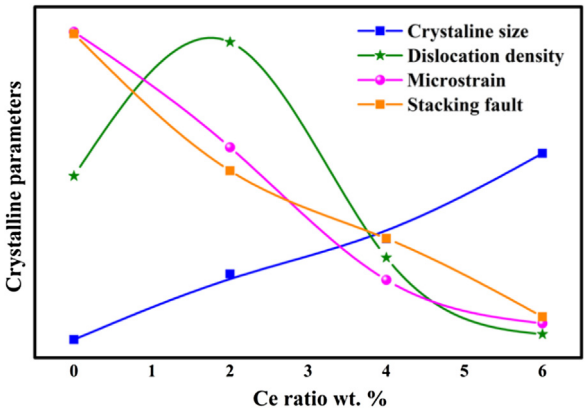

Fig. 3. Crystalline parameters of pure and Ce doped (x) wt. %.

3. Results and discussion

3.1. Structural parameters investigation

Fig. 2 illustrates the XRD pattern of the Ce-V_2O_5 films coated at 2500 rpm with (2–6 wt %) cerium concentrations and annealed at 500 °C. The diffraction pattern and corresponding miller indices (*hkl*) 2θ° are 12.41, 18.96, 25.02, 31.14, 31.45, 50.62 and 54.94 are (200), (221), (400), (233), (242), (046) and (464) planes. The observed XRD patterns of the films were compared with the standard International centre for diffraction data [ICDD = 45–1074]. It confirmed the tetragonal crystal phase of the films with highly preferential orientation along (221) direction. Fig. 2 (b–d) illustrates that the observed peak (221) position has shifted towards lower angle side (2θ° = 18.96 to 18.09) when Ce concentration is increased. This confirms the successful infusion of Ce into the V_2O_5 lattice site. Moreover the shift might be attributed to the higher ionic radius of Ce^{3+} (1.03 Å) compared to that of V^{5+} (0.59 Å) [8]. This variations may influence the crystalline parameters of the host lattice. The other orientations corresponding to (200), (400), (233), (242), (046) and (464) directions are presented with relative low by intensities when compared to (221) plane. This confirms that the crystalline growth is along (221) direction with an improved crystalline nature of the Ce-V_2O_5 films [9]. The crystalline parameters calculated the V_2O_5 films and are for list in Table 1. Evidently, the crystallite size (D) of the films were found to increase gradually with higher Ce concentration (2–6 wt%) due to the greater ionic size of cerium than that of vanadium. Generally, an improved grain size suggests a better-quality crystalline nature and reduction of grain boundary fraction in the films, which can minimum grain limit dispersion and therefore transport electrical resistivity [10]. In addition, owing to the removal of defects in the lattice with the addition of higher cerium concentration, the strain and dislocation density in the films get released [10]. This is as we have obtained a minimum value of strain and dislocation density for the higher concentration of Ce (6 wt%). Notably, the higher average crystallite size of 63.32 nm was recorded 6 wt% of Ce. It was calculated using the Debye Scherer's formula [11].

$$D = \frac{k\lambda}{\beta \cos\theta} \tag{1}$$

where, k-is constant value (0.9), λ-is incident beam wavelength, β-is FWHM of peak and θ-is an angle of XRD diffraction position. The micro-strain, dislocation density and stacking fault of coated V_2O_5 films were calculated using the following Eqs. (2–4).

$$\varepsilon = \beta \frac{\cos\theta}{4} \tag{2}$$

$$\delta = \frac{1}{D^2} \tag{3}$$

$$SF = \left[\frac{2\pi^2}{45\left(3\tan\theta\right)^{\frac{1}{2}}}\right]\beta \tag{4}$$

Fig.3 illustrates a variation of micro-strain, dislocation density and stacking fault with different doping concentration (2–6 wt%). The calculated crystalline parameters for Ce doped films decrease with increasing Ce concentration when compared to pure films, to the influence of Ce dopant on the V_2O_5 lattice. Especially, dislocation density value (3.85 to 1.37 × 10^{15} lines/m^2) of films decreased with increasing Ce concentration. The films with 6 wt.% of Ce revealed a minimum average value of microstrain and stacking fault (0.75 and 0.1510 × 10^{-2}) owing to the removal of defects in the lattice due to higher doping concentration of Ce, improved crystallinity and of the quality film [10,12]. From these results, we observe that small changes in Ce concentration of V_2O_5 films has discreetly affected the crystalline parameters and improved the crystallite size of Ce doped V_2O_5 films.

3.2. Surface morphology (FE-SEM) investigation

Fig. 4 illustrates the FE-SEM micrographs of the Ce-V_2O_5 films with different Ce doping concentration. The pure V_2O_5 films displayed rod-like structures with average diameter of ~55 nm [13] Interestingly, N. S. Kumar et al. [14], also observed a nanorod-like structures in V_2O_5 films at nanoscale regime [15]. Nanorodes with tiny nanoplates were observed after adding 2 wt.% of Ce concentration. The 4 wt.% of Ce displays both nanorods and nanoplate-like structures which are irregular shaped. Minimum amount of nanorods were transformed in to nanoplate-like structures. Interestingly, with 6 wt.% of Ce 90 % of nanorods are transformed in to nano plate-like structure with uneven shape. It is evident from the surface morphology changes that the crystallite size has increased. This surface changes will enhance the electrical properties of the V_2O_5 films. Similar Ce as a dopant and it exhibited nanoplate-like structure has been observed by R. Mariappan et al., [16]. Moreover, nanoplate-like structure can enhance the photo responsivity of the device due to it's superior surface to volume ratio of the V_2O_5 films [17]. FE-SEM of V_2O_5 films are supportive with XRD results. Evidently Ce with 6 wt. % in V_2O_5 doped film will

Table 1
Crystaline parameters for pure and Ce-V_2O_5 films.

Ce (wt. %)	Crystallite size(nm) (D_{ave})	Dislocation density × 10^{15}lines /m^2 (δ_{ave})	Micro strain (ε_{ave})	Stacking fault × 10^{-2} (SF_{ave})
0	42.07	3.85	1.211	0.1752
2	49.55	5.95	1.030	0.1635
4	53.56	2.57	0.822	0.1577
6	63.32	1.37	0.754	0.1510

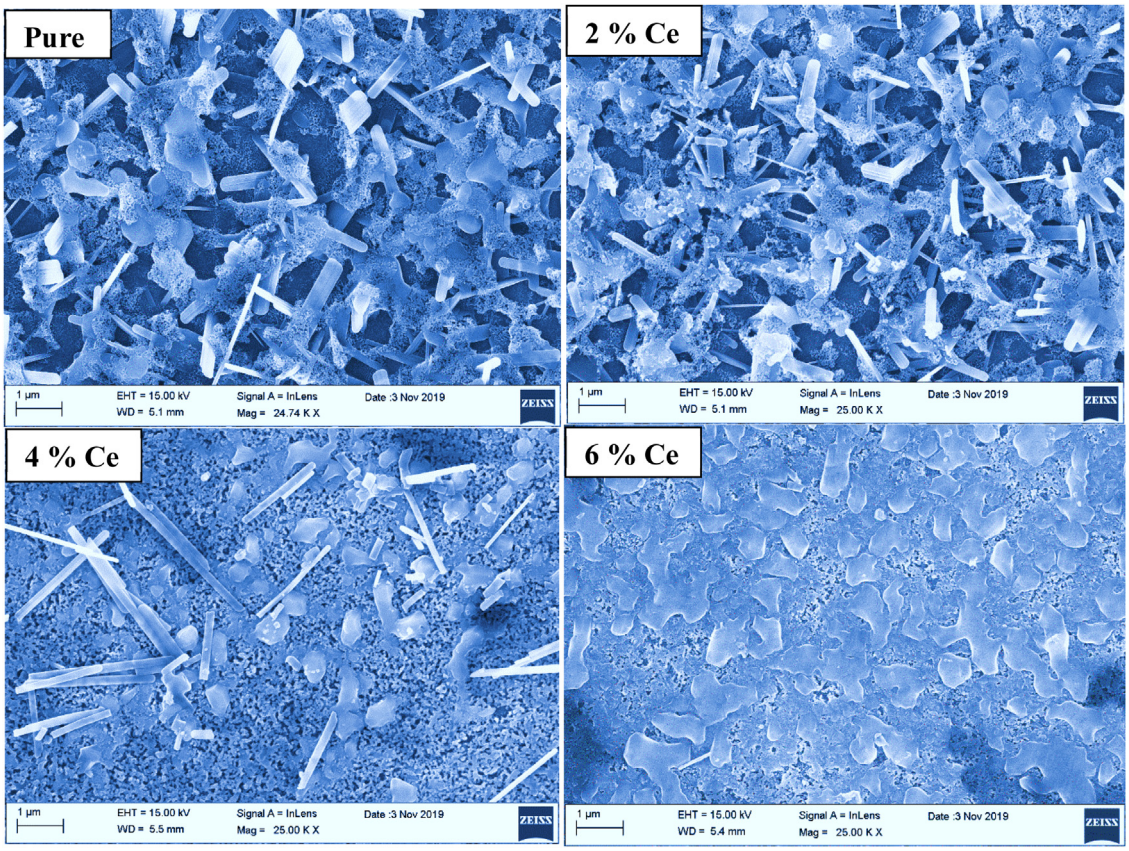

Fig. 4. FE-SEM images of pure and Ce doped (x) wt. %.

be appropriate interfacial layer for the device fabrication for photo electronic applications.

3.3. Surface roughness analysis (AFM) investigation

AFM images of Ce doped V_2O_5 films with different Ce concentration (2–6 wt%) scanned at 5 µm × 5 µm areas are displaced in Fig. 5. Generally, AFM images are used to the surface morphology information of the coated films, which is helpful to investigating the surface roughness and nature of the grains. The Root Square (RMS) for roughness can be calculated using the following relation.

$$\mathrm{RMS} = \sqrt{\frac{1}{N}\sum_{i=1}^{N} Z_i^2} \tag{5}$$

where N-is the total number of pixels probed and Zi is the height deviation in relation to the mean height of the surface films.

The calculated RMS values are 104, 98, 77 and 53 nm, for 2, 4 and 6 wt% of Ce, which indicate that the surface of the Ce doped V_2O_5 films is fairly smooth surface increased. This reduction in roughness occurs with the variation in crystallite size as evidenced from XRD study. This RMS values confirms the formation of a uniform layer of the Ce-V_2O_5 on n-Si surface which would favour the diode fabrication [18,19]. Prior reports by C.V. Prasad et.al., P.P. Thapaswini et.al., and V.R. Reddy et.al., reported that samples with fairly smooth surface showed better diode performance [18–20]. The film with 2 wt. % of Ce shows a sharp needle and rod-like structures, which are arranged more closely over the surface of the film. The grain shape changes to hillocks-like structures for 4 and 6 wt% Ce Concentration in V_2O_5 films. This is because the surface diffusion of atoms have a significant role in the reorganisation of the particles into a layer of elongated sheets [4,21]. Interestingly, M.M. Margonia et al [22] reported a similar change of surface structures, where the rod-like structures transform into hillocks structure and also the phenomenon of decreasing surface roughness of the V_2O_5 films. Moreover, the agglomeration of shoulder to shoulder nanorods leadings to the formation of microspheres [23]. In the fabrication of Schottky diode interfacial layer thickness play a vital role. The thickness of the V_2O_5 films increased with Ce concentration Table 2.

Table 2
Surface roughness of pure and Ce-V_2O_5 films.

Ce ratio wt. %	2	4	6
Surface roughness (nm)	63	67	45
RMS value nm	98	77	53
Thickness (nm)	579	587	595

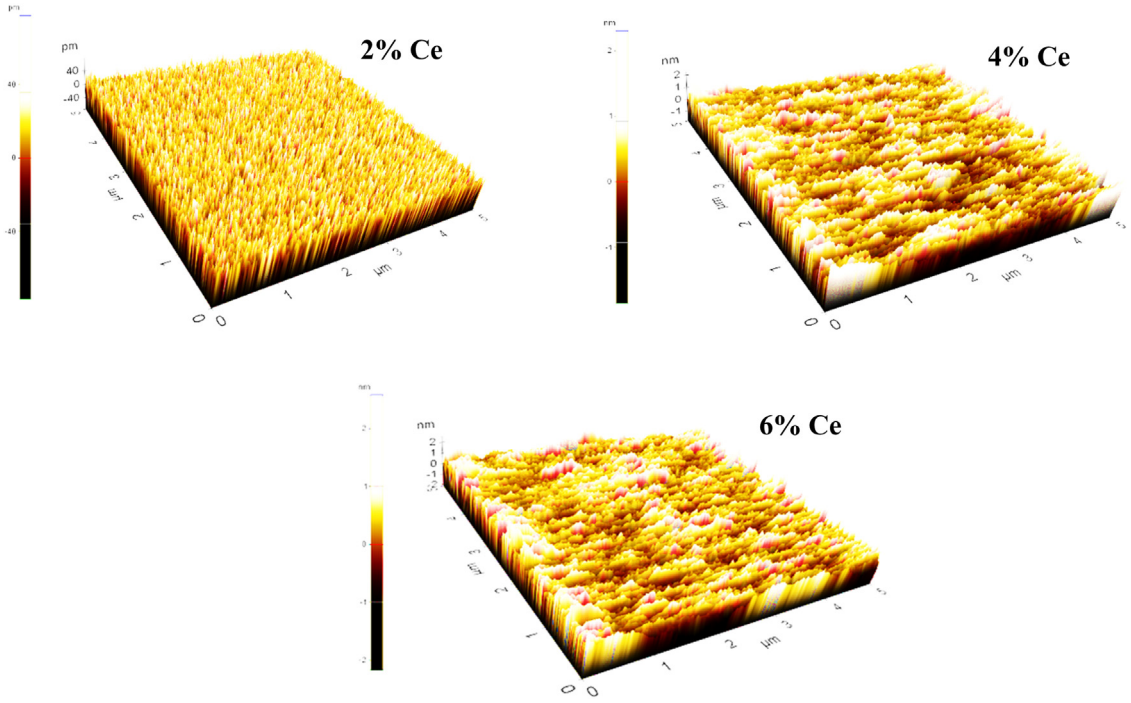

Fig. 5. AFM illustrate picture of pure V_2O_5 with different doping concentration of Ce.

Table 3
Atomic ratio of the pure and Ce-V_2O_5 films under different concentrations.

Ce wt. %	Atomic ratio (%)		
	Ce	V	O
0	-	16.51	83.49
3	2.99	16.83	80.18
6	3.70	16.28	80.02
9	5.97	15.73	78.30

Higher film thickness is obtained for 6 wt.% of Ce, which suggests that the Ce concentration improve the film thickness. Thickness of the film can be effortlessly controlled by various parameters in spin coating technique such as coating time, RPM/mints, the volume of solution and annealing time etc., The calculated RMS value, surface roughness and film thickness were tabulated in Table 2, which clearly indicate the V_2O_5 film with 6 wt. % of Ce has is considerably smooth surface, low surface roughness and RMS value with better film thickness when compared to other Ce-V_2O_5 films. These results might facilitate to improve the rectifying nature of MIS junction and Schottky diode parameters.

3.4. Elemental (EDX) investigation

Fig. 6 illustrates the EDX spectrum of pure and Ce doped V_2O_5 films with different concentration (2–6 wt%). The spectrum confirms the presence of expected elements like vanadium (V), Cerium (Ce) and oxygen (O). No other foreign elements are present in EDX spectrum, assuring the purity of the films. With increase in cerium concentration, the atomic percentage was found to be decrease regularly up to 6 wt.% was noted to be the minimum atomic percentage of O when compared with other films. Table 3 displays the constituent atomic percentage of the pure V_2O_5 films and Ce-V_2O_5 films. Results are one of the evidence to the stronger presence of Ce in V_2O_5 films. The higher Ce concentration offered a minimum amount of oxygen content which further showed a less defects, good crystallinity, and better electrical conductivity with lowest bad gap, for the V_2O_5 films.

Table 4
Optical parameter of pure and Ce doped (x) wt. %.

Ce wt. %	Absorption coefficient $\times 10^7$ $(cm)^{-1}$	Extinction coefficient	Optical band gap (eV)
0	1.38216	0.5499	3.27
2	1.3709	0.5460	3.10
4	1.5949	0.6346	3.05
6	1.7030	0.6776	2.99

4. Optical property

To further investigate the coated thin films, we have studied the optical properties of V_2O_5 doped films by UV–vis spectroscopy. The optical properties, such as absorbance and band gap of films play a crucial role in optoelectronic device applications.

4.1. Absorbance (A)

Fig. 7 illustrates the absorbance spectrum of V_2O_5 doped films for the wavelength ranging from 200 to 900 nm. Absorbance of the films has swelling with Ce concentration (2–6 wt %) owing to the increase in film thickness. V_2O_5 films show cut-off wavelength at around 360 nm and this edge exposed a good crystalline quality of the prepared films [24]. Film thickness is one of the key aspects, influencing optical property. Table 4 displays Ce doping concentration, variation band gap E_g and optical parameters. Pure and Ce doped V_2O_5 films show almost constant absorption in the UV–vis region. Besides, films demonstrate unmistakable damping owing to the high thickness and density of the free electrons [11]. Notably, 6 wt.% of Ce doped V_2O_5 film displays the maximum absorbance due to the high crystalline size and smooth surface which is comparatively higher than other V_2O_5 films, as confirmed by XRD and AFM images, respectively. Similar behaviour of Ce was also reported by R. Marandu et.al in Ce-WO_3 films [6]. Moreover, a film with high absorbance will be highly suitable for photovoltaic industrial applications especially as photo diode.

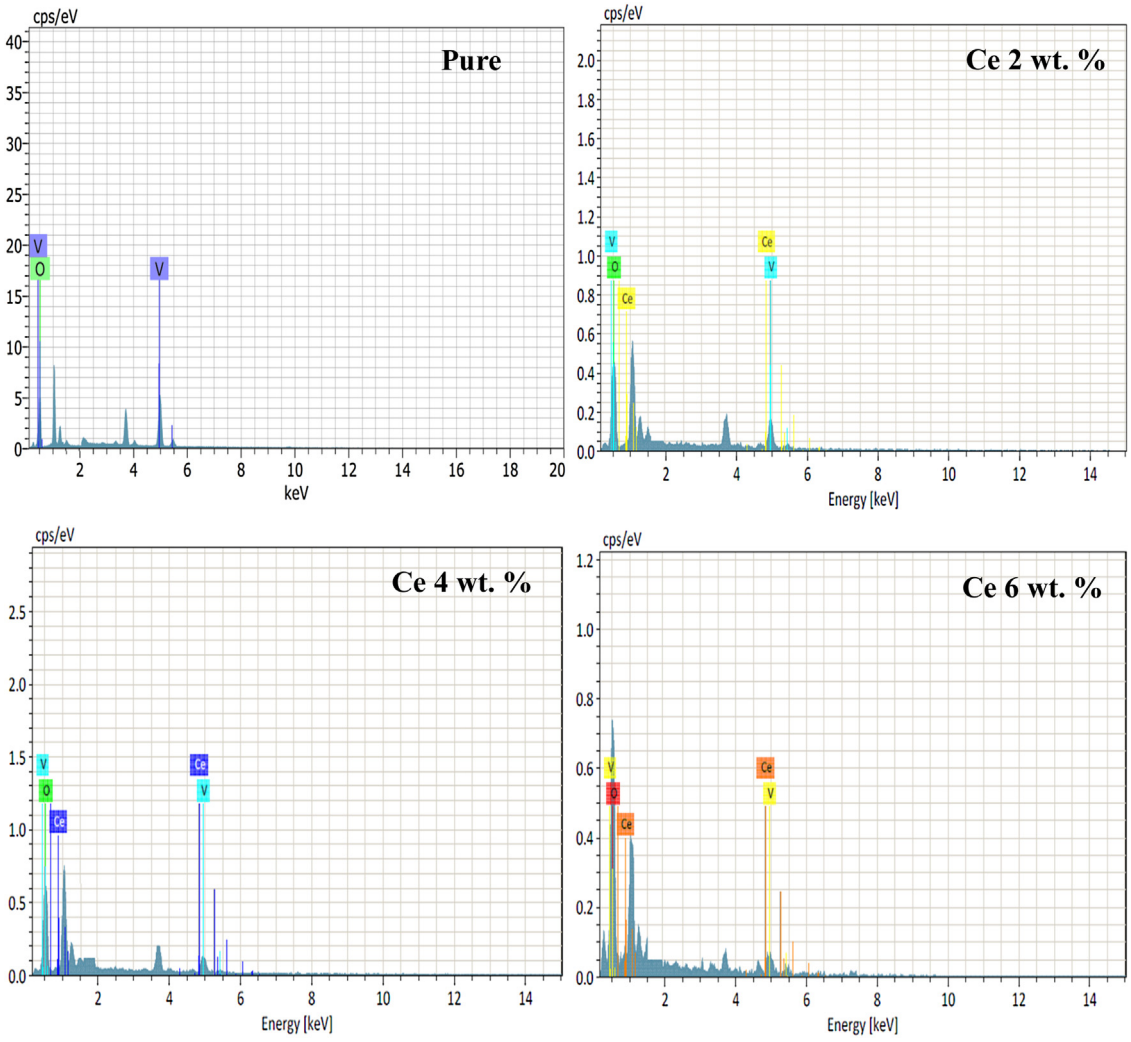

Fig. 6. EDX graph of Ce doped different contraction (x).

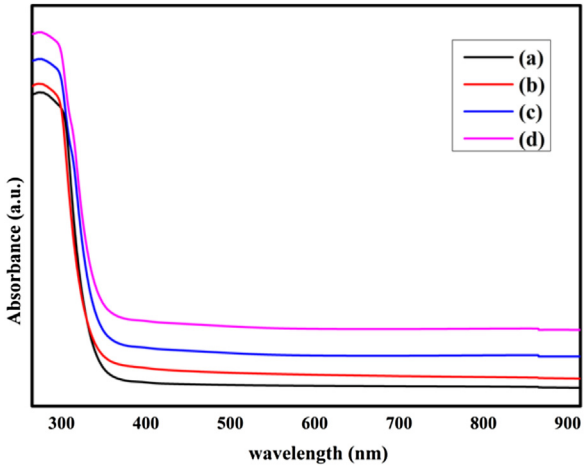

Fig. 7. Absorption graph pure and Ce doped (x) wt. %.

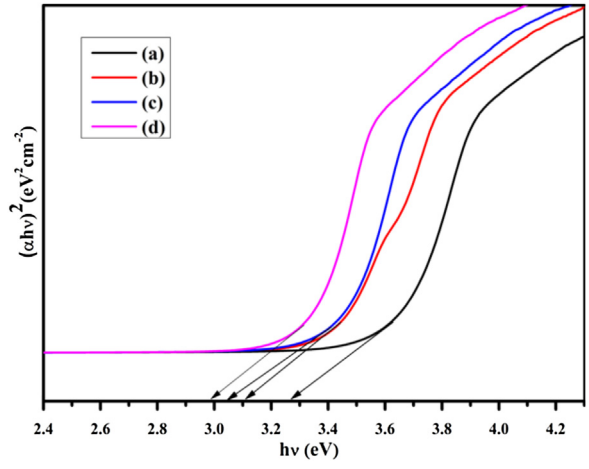

Fig. 8. Tauc's plot of pure and Ce doped (x) wt. %.

4.2. Optical energy gap (E_g)

Fig. 8 illustrates optical energy gap values of pure and Ce doped V_2O_5 films. The band gap values are estimated by extrapolating straight line in Taue's plot and using the flowing relation.

$$(\alpha h\nu)n = B(h\nu - Eg) \quad (6)$$

Where, n = 2 direct transition, α is the absorption co-efficient, hυ is the incident photon energy, B is the constant and Eg is the optical band energy of the films. Usually, crystal momentum of electrons and holes of the direct band gap materials are the same in both conduction and valance band [24]. Clearly, when an electron directly emits the photons it is one of advantages for the photoelectric

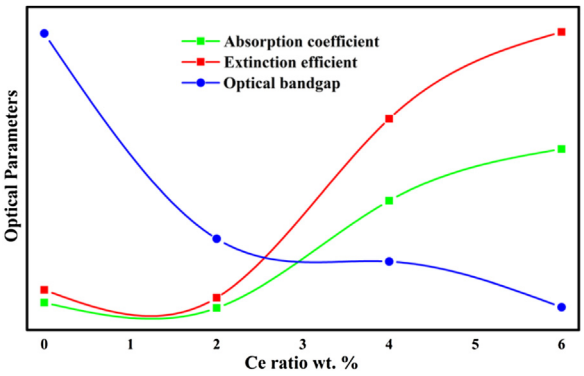

Fig. 9. Optical parameters of pure and Ce doped (x) wt. %.

device applications [24]. We have also calculated the important optical parameters like absorption co-efficient (α), extinction coefficient (κ) using the following relation:

$$\alpha = \left(\frac{1}{d}\right) \ln\left(\frac{1}{T}\right) \quad (7)$$

$$K = \frac{\alpha\lambda}{4\pi} \quad (8)$$

where T is the transmittance, d is the thickness of the film, α is the absorption coefficient and K is the extinction coefficient. Fig. 9 shows the changes of optical parameters for pure and Ce doped V_2O_5 films. The optical band gap values calculated by intercepts of the plots are found to be 2.99, 3.05, 3.10 and 3.27 eV consistent for Ce doped (0,2,4 and 6) concentration respectively. The absorption coefficient 1.7030 × 10^7 $(cm)^{-1}$ and extinction coefficient 0.6776. E_g of 6 wt.% Ce-V_2O_5 film considerably lesser than other V_2O_5 film. A similar trend was previously observed by M.A.M. Ahmed et al [12] and A.A. Dakhel et al., [25]. This different band gap values for undoped V_2O_5 and Ce doped films may be due to the following reasons (i) increase in film thickness as well as density of localized states near the band edges. (ii) Line or planar defects in the crystalline film and the crystalline size effect [4]. Eg values decrease on increasing the Ce doping concentration, which is related with the variation of peak shift in the absorption spectrum, red shift phenomena as well as quantum size effect and quantum confinement effect [26]. This widening optical band gap values could be due to the well-known Moss-Burstein effect [27]. Moreover, the narrowing of band gap comes as a consequence of the change in nature and strength of the crystalline potential by additional influence of Ce impurity dopant including the effect of their 4f-electrons on the crystalline electronic states [28]. Thus, due to the doping, the band tailing or impurity band becomes broader and finally reaches to merge at the bottom of the conduction band causing a decrease in the effective optical E_g. In addition, the surface structure, oxygen deficiency and crystallize size has also been reported as the reasons behind the band gap reduction [26–28].

5. Electrical property

5.1. DC electrical conductivity

The electrical conductivity (σ_{dc}) of the films were measured using Keithley electrometer with two probe setup. A voltage of 10–100 V was kept constant, while the electrical conductivity was measured for different temperatures (with the help of PID controlled oven) ranging from room temperature to 150 °C at a rate of 20 °C interval. I–V characteristics of the V_2O_5 and Ce- V_2O_5 thin films with (0, 2, 4 and 6) concentration presented in Fig. 10. The σ_{dc} can be calculated by the following equation. Fig. 11

Table 5
Electrical parameters for pure and Ce-V_2O_5 films.

Ce wt. %	Resistivity (Ω cm)	Conductivity (S cm−1)	Activation energy (eV)
0	1.2109×10^9	9.11×10^{-10}	0.07477
2	8.49×10^{14}	1.02×10^{-9}	0.13368
4	4.62×10^{12}	2.03×10^{-9}	0.08315
6	3.45×10^{12}	2.43×10^{-9}	0.06291

$$\text{Electrical conductivity}\,(\sigma_{dc}) = \left(\frac{I}{V}\right) \times \left(\frac{d}{A}\right) \text{ S/cm} \quad (9)$$

where I-is the output current, V-is the applied input voltage, d-is the inter-probe distance of two probe setup and A-is the cross-sectional area of the pure V_2O_5 and Ce-V_2O_5 films. The calculated electrical conductivity, resistivity and activation energy values were listed in Table 5. The calculated conductivity is found to in the range from 9.11 × 10^{-10} to 2.43 × 10^{-9} S/cm with different Ce concentrations. It is clear that the resistivity (8.49 × 10^{14} to 3.45 × 10^{12} Ωcm) also decreases while increasing Ce concentration (2–6 wt%) owing to good homogeneity and better hoping of electrons in the films [29,30]. The decline resistivity values of V_2O_5 films with Ce contraction is because the cerium exceeds the limit of maximum solubility in the V_2O_5 host lattice, inducing a grain boundary separation of impurities leading to the dispersion of charge carriers [31]. The obtained σ_{dc} values are more suitable to fabricate MIS type Schottky device. The activation energy (E_a) minimum amount of energy that is required to activate the atoms of the films were calculated from the Arrhenius plot using the following equation [32].

$$\text{Activation energy (Ea)} = \text{slope value X}\left(\frac{K_B}{e}\right) \text{ eV} \quad (10)$$

where, K_B-is the Boltzmann constant and e-is the electron charge. The V_2O_5 coated films vary from 0.07477 to 0.06291 eV with (0–6 wt%) of Ce doping concentration. These varation are due to the films thickness, defect of a crystal lattice, surface films and better hopping of electrons [33,34]. Doping includes a substitution of Ce ions in the V_2O_5 lattice, which liberates more conduction electrons in the conduction band [35]. Notably, Ce doped with 6 wt.% has minimum amount of activation energy with higher conductivity for V_2O_5 films. Furthermore, the smooth surface of the film with minimum crystal defects and good optical property could possibly enhance the MIS type photo-diode parameters compared to other doping concentrations of Ce. The addition of Ce ions have efficiently improved the electrical behaviour of the Ce-V_2O_5 f

5.2. Photo diode performance of Cu/Ce-V_2O_5/n-Si MIS structure diode

I–V characteristics were performed for analysing the diode parameter likes ideality factor, barrier height and photo-diode performance of the fabricated Cu/V_2O_5/n-Si structured Schottky diodes. V_2O_5 films with different wt. % of Ce is used as interfacial layer in the diodes. Fig. 12 (a, b) illustrates the schematic representation of the Cu/Ce-V_2O_5/n-Si MIS structured Schottky diode. Historically, the structure of the MIS diode and feasible energy level band structure with metal work function, interface states, electron affinity, Fermi level (E_F), conduction level (E_C) and the barrier height (Φ_B), are displayed in Figure. Generally, Fermi levels at metal/semiconductor interfaces are normally pinned due to metal induced gap states [36]. In fact, at the direct metal semiconductor contact, metal wave function decays into the semiconductor and creates metal induced gap states that results in Fermi level

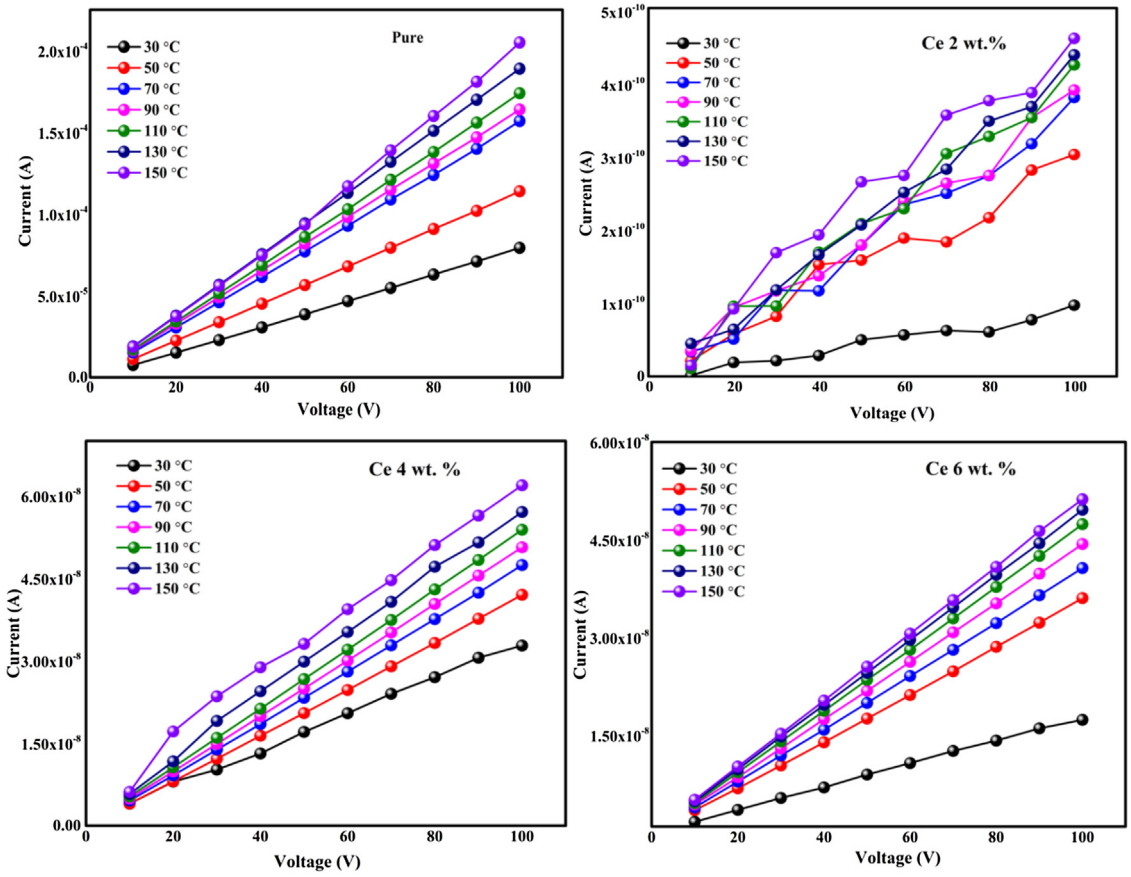

Fig. 10. I–V characteristics of of pure and Ce doped (x) wt. %.

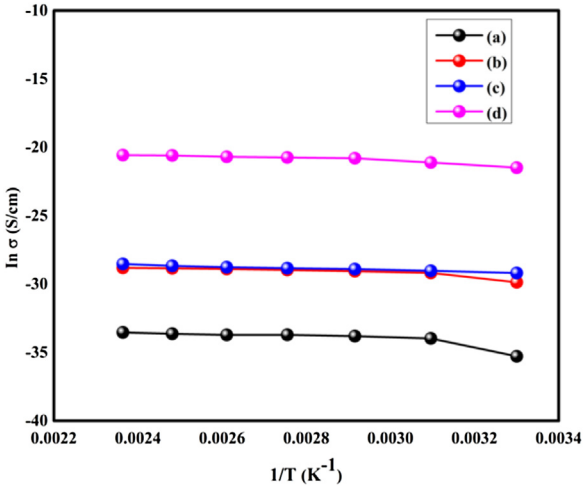

Fig. 11. Arrhenius plot of pure and Ce doped (x) wt. %.

pinning at the interface [37,38]. This may be the reason that the free-states are directly diffused into the metal to the semiconductor at the interface. However, insulating layer can reduce the Fermi level pining caused by metal induced gap states by suppressing the metal wave function penetration into the semiconductor band gap and also by Passivation of the free-states [39]. In the present work, Fig. 12 (b) Ce-V_2O_5 acts as an insulating layer blocking the free-states at the real MIS interface. Thus, it moderately increases the effective barrier height (BH) for the Cu/Ce-V_2O_5/n-Si MIS structured Schottky device. The interfacial layer thickness of the MIS type diode also play a dual role: it is semi-transparent for electrons moving from the metal to semiconductor, which ensures favourable conditions for efficient minority carrier injection, and blocks the hole current. Such a unique feature gives the possibility to suppress high leakage currents which are unavoidable in meta-semiconductor Schottky contacts [40,41]. Fig. 13 illustrates the I–V characteristic of fabricated diode measured under dark and light condition. The semi-logarithmic plots of MIS structured Schottky diode is given in Fig. 14. The forward and reveres bias I–V characteristic of the diode were measured by applying voltage ranging from +4 to −4 V. The current conduction mechanism of the Cu/Ce-V_2O_5/n-Si diodes were studied by thermionic emission theory using following equations [42].

$$I = Io\,[\exp(qV/nkT) - 1] \tag{11}$$

Where I_o is the reverse saturation current, q is electron charge, V is the applied voltage, n is the ideality factor, k is the Boltzmann constant and T is absolute temperature.

The barrier height (Φ_B) and ideality factor (n) are highly sensitive parameters affecting the device performance it can be calculated by the following relation [43].

$$\text{Ideality factor}(n) = \frac{q}{K_B T}\frac{dV}{d(\ln I)} \tag{12}$$

$$\text{barrier height}\,(\phi_B) = \frac{K_B}{q}\ln\left(\frac{AA^{*}T^2}{I_0}\right) \tag{13}$$

The fabricated MIS structured Schottky diode shows that the calculated ideality factor (n) values are not equal to one and if n equals one, pure thermionic emission happens but n is usually greater than unity. Upon doping, the V_2O_5 ideality factor decreases and barrier height increases as depicted in Table 6. This indicates

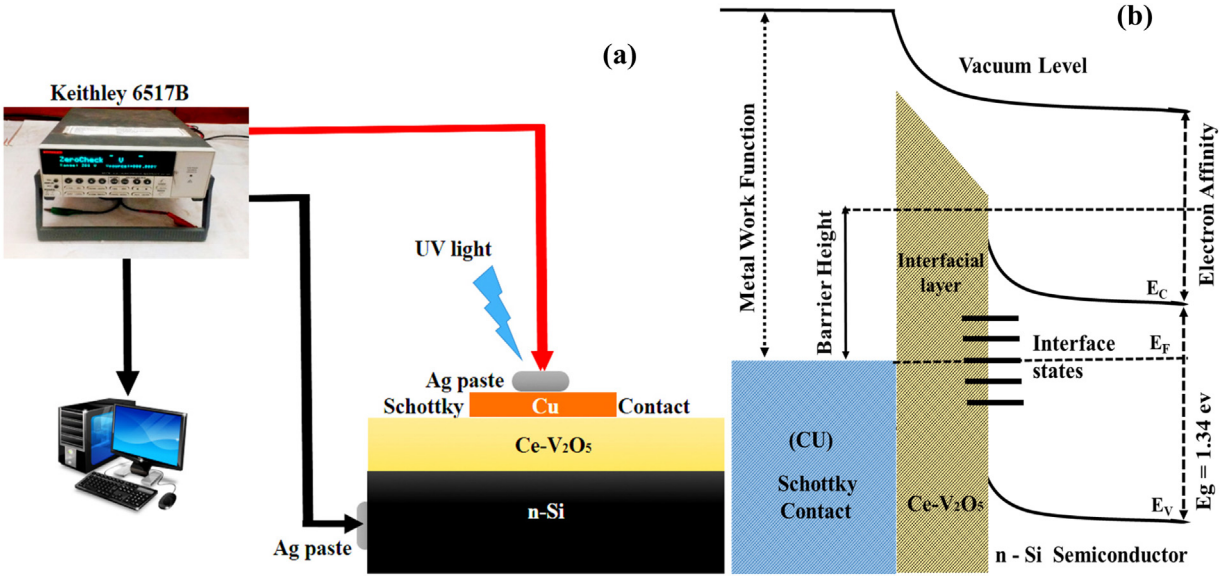

Fig. 12. (a) schematic illustration of MIS SBD's (b) Energy level band illustration of the Cu/Ce-V_2O_5/n-Si MIS SBD's interfacial layer and interface states.

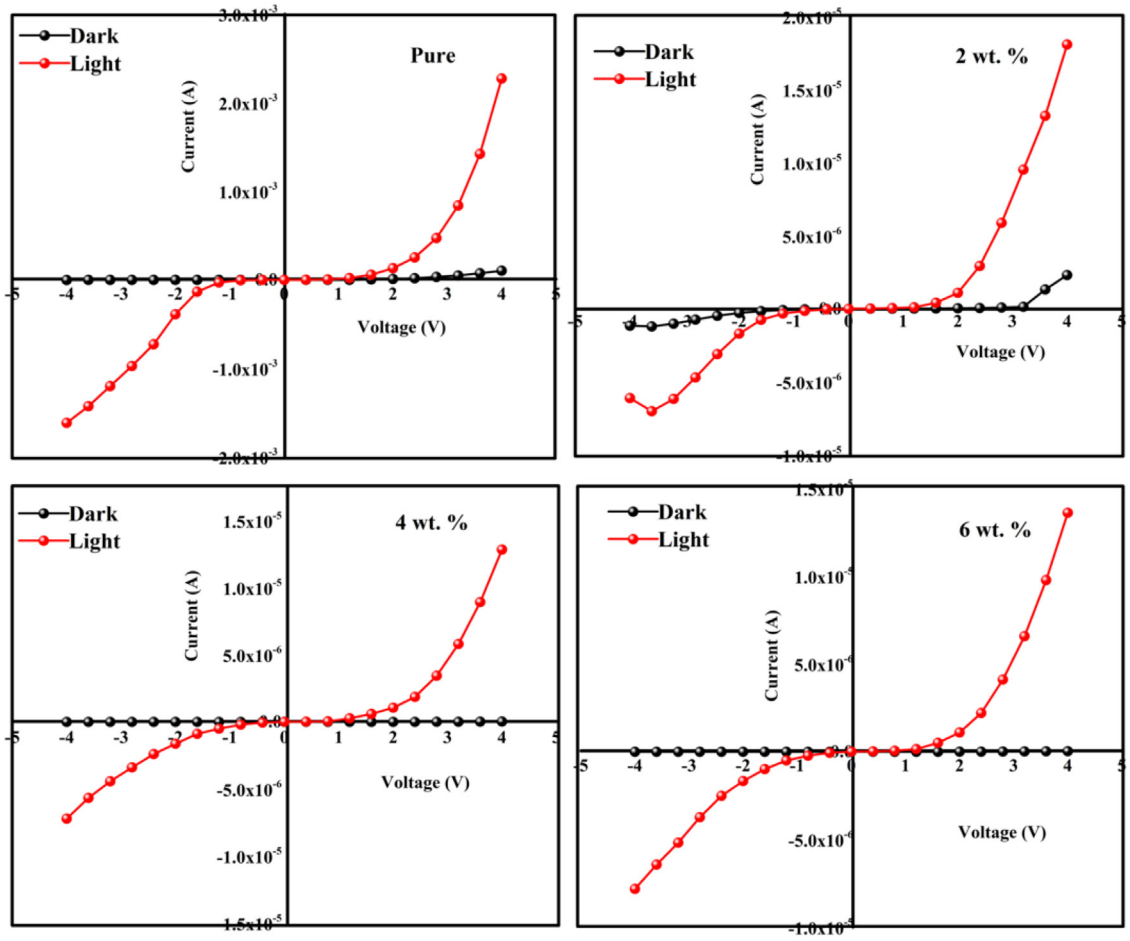

Fig. 13. I–V characteristics of Cu/Ce-V_2O_5/n-Si structured Schottky device with Ce contraction (x) wt.%.

that the doping concentration affectes the electrical properties thus improving the diode performance. A high ideality factor which is bigger than one could be attributed to various things in the diode for instance interface states, non-uniformity distribution of the interfacial charges, recombination-generation, series resistance, tunnelling effect, image force effect, additional capacitance, voltage drop present at the insulating layer and possibilities may be the presence of inhomogeneity barrier height [44,45]. Our n value is very small and can be compared to literature [28]. Results indicating that the insertion of the rare earth ions produces (Ce-V_2O_5)

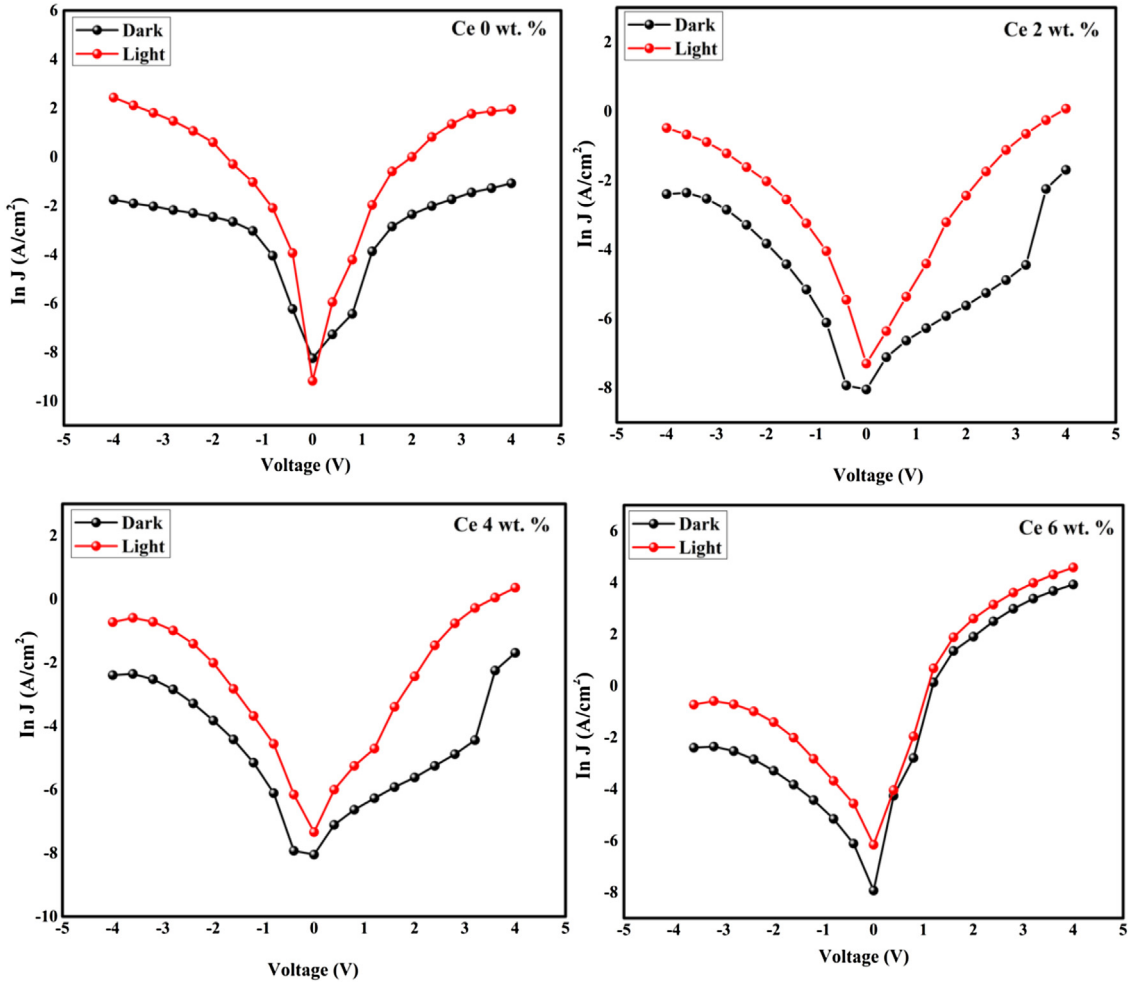

Fig. 14. Semi-logarithmic plots of MIS structured Schottky device with Ce doped (x) wt. %.

Table 6
Photodiode parameters like n, Φ_B, I_0, P_s, R, QE and D* are tabulated.

Ce (wt.%)	ϕ_B(eV)		n		Light condition				
	Dark	Light	Dark	Light	Current gain (g)	Photo-Sensitivity P_s (%)	Responsiviy R (mA/cm^2)	Quantum efficiency QE (%)	Detectivity D* Jones
0	0.66	0.67	6.95	5.09	20.70	748.82	13.38	5.97	8.87×10^9
2	0.69	0.70	3.97	3.78	27.45	2071.23	24.92	8.13	9.87×10^9
4	0.74	0.77	2.39	2.13	35.80	65543.46	36.38	14.20	1.99×10^{10}
6	0.79	0.82	1.95	1.73	48.90	96090.78	65.86	25.54	2.99×10^{10}

interlayer leading to a reduction of the ideality factor (n), increase barrier height (Φ_B) and decrease in the saturation current (I_0) values. Predominantly Ce 6 wt.% produce high I–V performance with better n = 1.73, Φ_B = 0.82 and (I_0) 5.06×10^{-4} values.

The photodiode performance were evaluated using parameters like Photo-sensitivity (PS), Responsivity (R), Current gain (g), Quantum efficiency (QE) and Detectivity (D*) for the Cu/V_2O_5/n-Si MIS SBD's. The photosensitivity of the diode can be calculated using the following reaction [6].

$$\text{Photosensitivity (PS\%)} = \frac{I_{Ph} - I_D}{I_D} \times 100 \quad (14)$$

where, I_{ph}- is photocurrent of the Schottky device and I_D is the dark current. Maximum photosensitivity of 96090.78 %, was obtained for the diode with 6 Ce wt.%. This may be due to the separation of electron-hole pairs at the junction corresponds to photo generated carriers light condition [6]. This value revel, that the fabricated diode is very sensitive under light condition, which will be more suitable for optical fibre communication systems.

The photo responsivity (R) of fabricated Schottky device can be calculated the following relation [46].

$$\text{Responsivity (R)} = \frac{I_{Ph}}{PA} \quad (15)$$

where, I_{ph}- is photocurrent of the Schottky device, P-is the input source optical power of the incident light sources and A-is the area of the Schottky device. The calculated responsivity of device values varied in of 13–65 mA/W with Ce concentration (2–6 wt%). Improved R value is owing to the higher surface to volume ratio of V_2O_5 films [47]. The photo-current values and responsivity of the diode is inclined on the crystalline nature of film because photo generation and recombination depends on the quality of film [48]. When Electron hole pairs are generated, the photo-generated holes diffuse to the surface of V_2O_5 films to trap more oxygen. Electron

hole recombination rate is reduced and the remaining free electrons exhibit longer lifetime, which increases the photocurrent and cause the photo response of the diode [47,48]. A higher responsivity of 65.86 mA/cm^2 was recorded for MIS Schottky diode with 6 wt % of Ce as interfacial layer, This is useful in high-speed operation diode.

The current gain (g) is defined as the ratio between the number of electrons collected per unit time in the dark to the number of absorbed photons required to create photoelectron per unit time [49] The current gain (g) of fabricated Schottky diode can be calculated using the following relation

$$\text{Current gain}\,(g) = \frac{I_{Ph}}{I_d} \tag{16}$$

where, I_{ph}- is photocurrent of the Schottky device at the light condition and I_d- is photocurrent of the Schottky device at dark condition. The calculated gain is found to be varying from 21 to 49 with different Ce concentration. The similar tendency was observed by V.N.M. Abd-Alghafour et al [49]. The Schottky barrier diodes with high current gain values are also used in high power applications, like Power rectifiers [48].

Quantum efficiency (QE) is an important parameter in the evaluation of the performance of a photodetector the number of charge carriers gathered to produce the photocurrent created for every number of incident light power on the fabricated device, which was calculated using the following relation [47]

$$\text{Quantum efficiency}\,(QE) = \frac{Rhc}{q\lambda} \tag{17}$$

where, h-is Planck's constant value, c-is the incident light velocity, q-is the electron charge and λ-is the wavelength of the light source. Generally rare earth ions enhance the luminance property, therefore quantum efficiency of the fabricated diode may increase with Ce concentration [49]. The high quantum efficiency was attained at 6 wt.% which also matching with the results of H.Y. Kim et.al., [50]. The MIS diode made with 6 wt%. Showed maximum QE of 25.34 %. which is more favourable for photodetector applications.

The equation for another key parameter of photodetectors application is detectivity (D) can be represented as the following equation [51].

$$\text{Detectivity}\,(D) = \frac{R}{(2qI_D)^{1/2}} \tag{18}$$

where, D is the detectivity, R is the responsivity, I_D is the dark current and q is the charge of an electron. As increase in doping concentration, the measured detectivity of the diode were found to be increased from 9×10^9 to 3×10^{10}Jones. Diode with high detectivity is most suitable for detecting a weak signal. It can be used in optoelectronic communication systems [51–55]. From the outcome of Cu/Ce-V_2O_5/n-Si Schottky device results, we conclude that the Ce concentration can strongly influnce the photodiode properties of the device. Predominantly Ce with 6 wt.% in V_2O_5 film is more suitable for the future design of modern photodetector application and optical fibre communication systems.

6. Conclusion

A highly sensitive Cu/Ce-V_2O_5/n-Si structured Schottky diode where effectively fabricated with various concentration Ce. The structure, optical and electrical properties of the interfacial layer (Ce-V_2O_5) where investigated through various technique. From structure analysis, the Ce concentration continually improved the crystallite size from 42.07 to 63.32 nm. Also, a tetragonal crystal structure was observed without any phase changes. The FE-SEM images showed a irregularly arrange nanorod and nanoplate-like structures. Incorporation of Ce ions reduce the surface roughness value of the V_2O_5 films. The minimum roughness value of 45 nm. Was recorded at 6 wt%. In UV–vis Study, the higher Ce concentration of 6 wt% exhibited maximum optical absorbance with lesser band gap 2.99 eV. The I–V characteristics of the Cu/Ce-V_2O_5/n-Si diode revealed a superior performance in under light condition. The diode with 6 Wt% achieved a remarkable photosensitivity of 96090.78 %. Which is 100 times higher than that of pure diode. Overall, the presence of Ce-V_2O_5 layer in between Cu/n-Si is more suitable for the development of MIS photo detector application.

Author statement

I am submitting the manuscript entitled "Colossal photosensitive boost in Schottky diode behaviour with Ce-V_2O_5 interfaced layer of MIS structure" by V. Balasubramani, J. Chandrasekaran, Tien Dai Nguyen, S. Maruthamuthu, R. Marnadu, P. Vivek, S. Sugarthi, to be published in your esteemed journal "Sensors and Actuators A: Physical" The manuscript is original and has been written by the stated authors, who are all aware of its content and have approved its submission. The article has not been published previously and is also not under consideration for publication elsewhere. There is no conflict of interests and, if accepted, the article will not be published elsewhere in the same form, in any language without the written consent of the publisher.

Declaration of Competing Interest

The authors report no declarations of interest.

Acknowledgments

Authors gratefully acknowledge Department of Science and Technology (DST), Government of India, for the financial support in the form of project (EMR/2016/007874).

Appendix A. Supplementary data

Supplementary material related to this article can be found, in the online version, at doi:https://doi.org/10.1016/j.sna.2020.112333.

References

[1] S. Mahato, J. Puigdollers, Phys. B Phys. Condens. Matter 530 (2018) 327.
[2] S. Beke,Thin Solid Films 519 (2011), 085313.
[3] K.D.A. Kumar, R. Thomas, S. Valanarasu, V. Ganesh, M. Shkir, S. AlFaify, J. Thirumalai, Appl. Phys. A Mater. Sci. Process. 125 (2019).
[4] B. Etemadi, J. Mazloom, F.E. Ghodsi, Mater. Sci. Semicond. Process. 61 (2017) 99.
[5] M.A.M. Ahmed, W.E. Meyer, J.M. Nel, Mater. Sci. Semicond. Process. 103 (2019).
[6] R. Marnadu, J. Chandrasekaran, S. Maruthamuthu, V. Balasubramani, P. Vivek, R. Suresh, Appl. Surf. Sci. 480 (2019) 308.
[7] M. Raja, J. Chandrasekaran, M. Balaji, B. Janarthanan, Mater. Sci. Semicond. Process. 56 (2016) 145.
[8] I.M. Ali, J.M. Rzaij, Q.A. Abbas, I.M. Ibrahim, H.J. Alatta, Iran. J. Sci. Technol. Trans. A Sci. 42 (2018) 2375.
[9] D. Vasanth Raj, N. Ponpandian, D. Mangalaraj, C. Viswanathan, Mater. Sci. Semicond. Process. 16 (2013) 256.
[10] L.L. Pan, G.Y. Li, J.S. Lian, Appl. Surf. Sci. 274 (2013) 365.
[11] M. Balaji, J. Chandrasekaran, M. Raja, Mater. Sci. Semicond. Process. 43 (2016) 104.
[12] M.A.M. Ahmed, W.E. Meyer, J.M. Nel, Mater. Res. Bull. 115 (2019) 12.
[13] V. Balasubramani, J. Chandrasekaran, R. Marnadu, P. Vivek, S. Maruthamuthu, S. Rajesh, J. Inorg. Organomet. Polym. Mater. 29 (2019) 1533.
[14] N.S. Kumar, M.S. Raman, J. Chandrasekaran, R. Priya, M. Chavali, R. Suresh, Mater. Sci. Semicond. Process. 41 (2016) 497.
[15] N. Senthil Kumar, J. Chandrasekaran, R. Mariappan, M. Sethuraman, M. Chavali, Superlattices Microstruct. 65 (2014) 353.
[16] R. Mariappan, V. Ponnuswamy, P. Suresh, R. Suresh, M. Ragavendar, A. Chandra Bose, J. Alloys. Compd. 588 (2014) 170.

[17] R. Marnadu, J. Chandrasekaran, S. Maruthamuthu, P. Vivek, V. Balasubramani, P. Balraju, J. Inorg. Organomet. Polym. Mater. (2019).
[18] C.V. Prasad, M.S.P. Reddy, V. Rajagopal Reddy, C. Park, Appl. Surf. Sci. 427 (2018) 670.
[19] P.P. Thapaswini, R. Padma, N. Balaram, B. Bindu, V. Rajagopal Reddy, Superlattices Microstruct. 93 (2016) 82.
[20] V. Rajagopal Reddy, V. Manjunath, V. Janardhanam, Y.H. Kil, C.J. Choi, J. Electron. Mater. 43 (2014) 3499.
[21] N. Balaram, V. Rajagopal Reddy, P.R. Sekhar Reddy, V. Janardhanam, C.J. Choi, Vacuum 152 (2018) 15.
[22] M.M. Margoni, S. Mathuri, K. Ramamurthi, R.R. Babu, V. Ganesh, K. Sethuraman, Appl. Surf. Sci. 449 (2018) 193.
[23] D.V. Raj, N. Ponpandian, D. Mangalaraj, C. Viswanathan, Mater. Sci. Semicond. Process. 16 (2013) 256.
[24] R. Suresh, V. Ponnuswamy, R. Mariappan, N. Senthil Kumar, Ceram. Int. 40 (2014) 437.
[25] A.A. Dakhel, Mater. Chem. Phys. 130 (2011) 398.
[26] F.A. Garcés, N. Budini, R.D. Arce, J.A. Schmidt, Procedia Mater. Sci. 9 (2015) 221.
[27] B. Benhaoua, S. Abbas, A. Rahal, A. Benhaoua, M.S. Aida, Superlattices Microstruct. 83 (2015) 78.
[28] M.A.M. Ahmed, W.E. Meyer, J.M. Nel, Mater. Sci. Semicond. Process. 87 (2018) 187.
[29] P. Vivek, J. Chandrasekaran, R. Marnadu, S. Maruthamuthu, V. Balasubramani, P. Balraju, Optik (Stuttg) 199 (2019).
[30] P. Vivek, J. Chandrasekaran, R. Marnadu, S. Maruthamuthu,Superlattices Microstruct. 133 (2019), 106197.
[31] M.S. Raman, N.S. kumar, J. Chandrasekaran, R. Priya, P. Baraneedharan, M. Chavali, Optik (Stuttg) 157 (2018) 410.
[32] R. Suresh, V. Ponnuswamy, R. Mariappan, Appl. Surf. Sci. 273 (2013) 457.
[33] R. Suresh, V. Ponnuswamy, R. Mariappan, Mater. Sci. Semicond. Process. 21 (2014) 45.
[34] R. Suresh, V. Ponnuswamy, C. Sankar, M. Manickam, R. Mariappan, Ceram. Int. 42 (2016) 12715.
[35] M. M, R.M.R. Suresh, V. Ponnuswamy, C. Sankar, RSC Adv. 6 (2016) 53967.
[36] K. Sasikumar, R. Bharathikannan, J. Chandrasekaran, M. Raja, J. Inorg. Organomet. Polym. Mater. 30 (2020) 564.
[37] K. Sasikumar, R. Bharathikannan, M. Raja, Silicon 1 (2018).
[38] K. Sasikumar, R. Bharathikannan, M. Raja, B. Mohanbabu,Superlattices Microstruct. 139 (2020), 106424.
[39] C. Venkata Prasad, V. Rajagopal Reddy, C.J. Choi, Appl. Phys. A Mater. Sci. Process. 123 (2017) 0.
[40] R.T. Tung, Mater. Sci. Eng. R Rep. 35 (2001) 1.
[41] D.A. Svintsov, A.V. Arsenin, D.Y. Fedyanin, Opt. Express 23 (2015) 19358.
[42] R. Marnadu, J. Chandrasekaran, M. Raja, M. Balaji, S. Maruthamuthu, P. Balraju, Superlattices Microstruct. 119 (2018) 134.
[43] R. Marnadu, J. Chandrasekaran, M. Raja, M. Balaji, V. Balasubramani, J. Mater. Sci. Mater. Electron. 29 (2018) 2618.
[44] I. Orak, A. Kocyigit, A. Turut, J. Alloys. Compd. 691 (2017) 873.
[45] M. Uma, V. Rajagopal Reddy, V. Janardhanam, C.J. Choi, J. Mater. Sci. Mater. Electron. 30 (2019) 18710.
[46] A.M. Selman, Z. Hassan, Mater. Res. Bull. 73 (2016) 29.
[47] N.K. Hassan, M.R. Hashim, J. Alloys. Compd. 577 (2013) 491.
[48] K.M. Chahrour, N.M. Ahmed, M.R. Hashim, N.G. Elfadill, M. Bououdina, Sens. Actuators, A Phys. 239 (2016) 209.
[49] N.M. Abd-Alghafour, N.M. Ahmed, Z. Hassan, M. Bououdina, Appl. Phys. A Mater. Sci. Process. 122 (2016) 1.
[50] H.Y. Kim, J.H. Kim, Y.J. Kim, K.H. Chae, C.N. Whang, J.H. Song, S. Im, Opt. Mater. (Amst) 17 (2001) 141.
[51] Z. Du, D. Fu, T. Yang, Z. Fang, W. Liu, F. Gao, L. Wang, Z. Yang, J. Teng, H. Zhang, W. Yang, J. Mater. Chem. C 6 (2018) 6287.
[52] S. Demirezen, S. Altindal Yeriskin, Polym. Bull. 77 (2020) 49–71.
[53] S. Altindal Yeriskin, J. Mater. Sci. Mater. Electron. 30 (2019) 17032–17039.
[54] V. Balasubramani, J. Chandrasekaran, V. Manikandan, R. Marnadu, P. Vivek, P. Balraju,Inorg. Chem. Commun. 119 (2020), 108072.
[55] R. Marnadu, J. Chandrasekaran, S. Maruthamuthu, P. Vivek, E. Vijayakumar, New J. Chem. 44 (2020) 7708–7718.

Biographies

V. Balasubramani is currently pursuing his doctoral degree in Department of Physics at Sri Ramakrishna Mission Vidyalaya College of arts and science, Coimbatore, India with specialization in material science. Previously, he earned BS, MS and master of philosophy degree in Physics from Periyar university, salem, India. His current research interests include thin film, MIS type Schottky diode photodetectors and semiconductor devices for optoelectronic application.

Dr. J. Chandrasekaran received his BS and MS degrees and Doctor of Philosophy in Physics from Madurai Kamaraj University, Madurai (India), He Currently working as Associate Professor and Head, Department of Physics, Sri Ramakrishna Mission Vidyalaya College of Arts & Science, Coimbatore India (Oct 1988 – Till date). His current research interests include Fabrication of Electronic Devices especially Solar Cell, semiconductor diodes and NLO Material Characterization

Nguyen Tien Daireceived the PhD degree in advanced materials science and engineering from Chungnam National University, South Korea, in 2018. Currently, he is working as a lecturer and researcher in materials science and engineering at Duy Tan University, Vietnam. His research interests are metal oxides, perovskite, epitaxial growth of semiconductors for the gas sensor, photocatalysts, optoelectronic devices (solar cell and infrared LED and photodetector) applications

Dr. S. Maruthamuthu received his BS and MS degrees in Physics from Bharathidasan University, India. He graduated with PhD degree in Material Science (DSSC) from Research and Development Centre, Bharathiar University, India. He has more than a decade of teaching experience in Material science and Engineering Physics and currently working as Associate Professor at PSG Institute of Technology and Applied Research, Coimbatore, India. His current research interests include Nano material synthesis for energy storage devices, thin film for photodetectors & solar cells.

R. Marnadu has received his B.Sc. degree in Physics from Madurai Kamaraj University, Madurai (India) and M.Sc. in Physics from Bharathiar University, Coimbatore (India). Currently he is pursuing Ph.D. in Physics at Department of Physics, Sri Ramakrishna Mission Vidyalaya College of arts and science, Coimbatore (India) with specialization in Material Science. His research interest focuses on the development of low-cost UV photodetector, MIS type Schottky structure, photo-diode, and thin film based semiconductor devices for optoelectronic application.

P. **Vivek** is presently working as Ph.D. scholar in the department of Physics at Sri Ramakrishna mission Vidyalaya college of arts and science, Coimbatore (India) with specialization in thin film and material science. Previously, he earned master of philosophy (M.Phil) degree in material science from periyar university salem (India). His current research interests include thin film photodetectors and solar cell.

Sugarthi Srinivasan is currently pursuing her doctoral degree in Functional Materials and Energy Devices Laboratory, Department of Physics and Nanotechnology, SRM Institute of Science and Technology, India. She received her UG and PG degree from Periyar University, Salem, India. She is working in Pt free counter electrode materials (Ag based ternary metal sulfides) for third generation solar cells. Her research interest includes toxic free catalytic materials for energy conversion and storage applications.